Efficient Broadband Triplet–Triplet Annihilation-Assisted Photon Upconversion at Subsolar Irradiance in Fully Organic Systems

Angelo Monguzzi, Sergey M. Borisov, Jacopo Pedrini, Ingo Klimant, Mario Salvalaggio, Paolo Biagini, Fabio Melchiorre, Camilla Lelii, and Francesco Meinardi**

The latest trend in solar cell technology is to develop photon managing processes that adapt the solar emission to the spectral range at which the devices show the largest intrinsic efficiency. Triplet–triplet annihilation-assisted photon upconversion (sTTA-UC) is currently the most promising process to blue-shift sub-bandgap photons at solar irradiance, even if the narrow absorption band of the employed chromophores limits its application. In this work, we demonstrate how to obtain broadband sTTA-UC at sub-solar irradiance, by enhancing the system's light-harvesting ability by way of an ad-hoc synthesized family of chromophores with complementary absorption properties. The overall absorptance is boosted, thus doubling the number of upconverted photons and significantly reducing the irradiance required to achieve the maximum upconversion yield. An outstanding yield of ≈10% is obtained under broadband air mass (AM) 1.5 conditions, which allows a DSSC device to operate by exploiting exclusively sub-bandgap photons.

1. Introduction

The photovoltaic effect has been turned into a technology to produce electricity from 1954, when a silicon-based p–n junction device showed a solar power conversion efficiency of 6%.[1] Since then solar cells (SC) gained in efficiency, found many applications in the consumer market, and actually represent the main clean and sustainable source of energy that meets global energy challenges.[2,3] However, SC efficiency is still limited by the spectral mismatch between the solar emission and the absorption spectrum of the employed semiconductors.[4] For instance, silicon-based devices are unable to exploit infrared photons at wavelengths longer than 1 µm, and this problem is even more relevant for organic SCs. Polymeric, single-molecule, and dye-sensitized solar cells (DSSCs) have been developed over the last years as a potential alternative to inorganic SCs because of their low production cost and great flexibility of use. However, the absorption of commercially available organic SCs has not been yet extended to the red/near-infrared portion of the solar spectrum below 700 nm,[5] wasting a number of photons equal to that available in the UV–vis range.[6] Similar considerations apply to photocatalytic water splitting cells (PCWS) for hydrogen production. This technology converts light into chemical energy and, thanks to its simplicity, is considered an attractive and challenging approach in green technological solutions for future global energy and environmental issues. However, sun-powered PCWS devices exploit only deep-blue/UV photons, while more than 95% of the solar radiation is lost.[7] In order to harvest low-energy photons, solar devices can be upgraded in different ways (multiple junctions cells, new chromophores, new photo-anodes, etc.), but all of them suffer from high fabrication costs or do not give rise to a significant enhancement of the efficiency. Therefore, the most recent trend in the field is to develop photon-energy managing processes to adapt the solar spectrum to the spectral range where the selected device is intrinsically highly efficient.[8] As sketched in **Figure 1**, this could be achieved by coupling SCs with optically active materials that are able to blue-shift the unexploited photons through several different processes of light upconversion (UC).[9] It has been estimated that the recovery of sub-bandgap photons could allow an improvement of organic SC performances of up to 50%,[3,10] and even larger increments, of up to 100%, are expected for PCWS cells.

Traditional UC methods rely on multiphoton processes (e.g., second-harmonic generation in non-linear crystals, or

Dr. A. Monguzzi, J. Pedrini, Prof. F. Meinardi
Dipartimento di Scienza dei Materiali
Università degli Studi Milano Bicocca
via R. Cozzi 55, 20125 Milan, Italy
E-mail: angelo.monguzzi@mater.unimib.it;
meinardi@mater.unimib.it
Dr. S. Borisov, Prof. I. Klimant
Institute of Analytical Chemistry and Food Chemistry
Graz University of Technology
8010 Graz, Stremayrgasse 9/II, Austria
Dr. M. Salvalaggio, Dr. P. Biagini, F. Melchiorre
Eni S.p.A. – Renewable Energy & Environmental R&D Center
Istituto Eni Donegani
via G. Fauser 4, 28100 Novara, Italy
Dr. C. Lelii[+]
Department of Physical and Chemical Sciences
University of L'Aquila
via Vetoio (Coppito 1) – 67100
L'Aquila, Italy
[+]Present address: Morgan Carbon Italia srl
Process Engineering Department
via Roma 338, 64014 Martinsicuro, Teramo, Italy

DOI: 10.1002/adfm.201502507

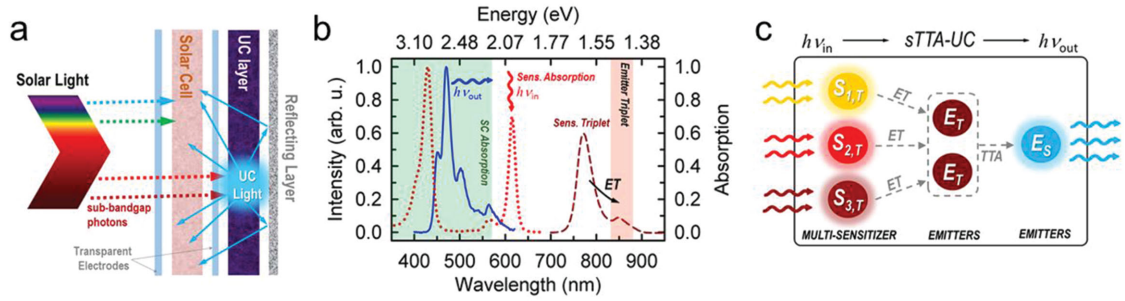

Figure 1. Operating principles of the photon upconversion through sensitized TTA. a) Sketch of a SC coupled to a sTTA-UC material for light harvesting enhancement. The transmitted sub-bandgap photons are blue-shifted by the UC layer, in order to be exploited by the SC. b) sTTA in a standard bi-component system. A sensitizer absorbs the incoming photons at an energy level below that of the SC absorption edge (dotted line, $h\nu_{in}$) and excites the optically dark emitter triplets (red stripe) via Dexter energy transfer (ET) from its phosphorescent triplets (dashed line). Upon triplet–triplet annihilation (TTA), upconverted photoluminescence is generated (solid blue line, $h\nu_{out}$) and absorbed by the SC (light-blue stripe). c) Outline of a multi-sensitizer TTA-UC system. Three sensitizers are excited simultaneously under white light illumination at different energies ($S_{i,T}$). All of them transfer the harvested energy to emitter triplets E_T, thus broadening the overall absorption of the system and increasing the number of emitter fluorescent singlets E_S generated upon TTA.

two-photon absorption in rare-earth doped materials),[11,12] which require high light intensities (up to MW cm^{-2}) that are well above the solar irradiance (≈100 mW cm^{-2}).[2] To achieve efficient conversion at low power, photon upconversion based on sensitized triplet–triplet annihilation (TTA) in organic bi-component systems (sTTA-UC) is investigated since it has been demonstrated under solar illumination in 2006. Briefly, a light-harvesting molecule, the sensitizer, absorbs low-energy photons and transfers the harvested energy to metastable triplet states of another molecule, the emitter. Through TTA, two excited emitters combine their energy to yield one emitter in a high-lying fluorescent singlet state, thus generating high-energy photons (Figure 1b and Figure S1, Supporting Information).[13,14] The rapid development of sTTA-UC materials led to conversion yields of >30% with non-coherent excitation at irradiance levels comparable to several suns (1 sun = 100 mW cm^{-2} under Air Mass 1.5 conditions),[15–21] and sTTA-UC has been used to enhance the light-harvesting capability of photovoltaic and PCWS cells, simply by placing the upconverter on the backside of the device to recapture a fraction of the sub-bandgap transmitted photons.[21,22] However, the improvements obtained with the currently available sensitizers are rather limited so far. To date, the best amongst the proposed sensitizers are phosphorescent metalated porphyrins, which have electronic properties suitable for i) efficient sensitization of the dark triplets of the highly fluorescent emitters used in sTTA-UC systems, and ii) prevention of re-absorption of upconverted light, thanks to their large transparency windows in the absorption spectrum (Figure 1b).[24] On the other side, the low-energy absorption peak of these porphyrins, which is exploited in the sTTA-UC, shows a typical bandwidth of 10–20 nm, allowing the harvesting of only a small fraction of the solar photons.[23] This is a crucial bottleneck, already faced in rare-earth based upconverters, that prevents the employment of sTTA-UC in real world applications.[12,26,27]

The broadening of the sensitizer absorption band it is not only required to increase the number of collected photons, thereby boosting the total light output, but also to decrease the irradiance required for having the highest sTTA-UC yield. Indeed, in these systems the conversion efficiency (QY_{UC}), defined as the ratio between the number of converted photons and that of the absorbed ones, depends on the steady-state density of emitter triplets, which is determined by the light-harvesting ability of the system. In general, QY_{UC} is rather low at low excitation powers. Then, it increases linearly with the irradiance up to the so called excitation power density threshold I_{th}, above which it rapidly saturates to its maximum value.[19] It is evident that, for applications in the SC technologies, I_{th} must be as low as possible and certainly below, or at least comparable, with air mass (AM) 1.5 solar irradiance. At present, this goal has only been accomplished in hybrid devices, obtained by coupling a layer of cadmium selenide fluorescent nanocrystals that serve as a booster for the sensitizer absorption to a sTTA-UC system. Drawbacks of this approach are a more complex device architecture, and the introducion of an additional photophysical step, which is intrinsically less efficient than a fully organic sTTA-UC with a comparable absorption spectrum.[28]

A promising strategy to extend the absorption of a sTTA-UC system consists in the simultaneous use of more sensitizers. This concept was proposed for the first time in 2007 by Baluschev and co-workers, who achieved NIR-to-vis conversion by exploiting two different sensitizers simultaneously excited by two lasers or by concentrated solar light (1 W cm^{-2}), and only recently the same group developed a broadband absorption system probably because of a lack of suitable dyes available on the market.[29,30] Here, we have taken this approach to the extreme by synthesizing a full set of sensitizers that were designed ad hoc, and in which each sensitizer is able to transfer the harvested energy to the same emitter. In this way, we obtained an optimized sTTA-UC system with a continuous and broad absorption, which allowed achieving a QY_{UC} as large as 10% under 1 sun of broadband non-coherent excitation light. This system, coupled to a model DSSC, demonstrated the feasibility of generating detectable electrical power at solar irradiance by exploiting only sub-bandgap photons.

2. Design and Fabrication of Broadband Absorption sTTA-UC Systems

Fluorescent polyacenes with emissions that match the absorption of SCs are generally employed as emitters. For this experiment, we used perylene (see Supporting Information, Figure S2), which is the ideal dye for this purpose thanks to its peculiar properties. First, its fluorescence quantum yield is close to that in diluted solution. Second, its triplet-to-ground state electronic transition is strictly forbidden, ensuring a triplet natural lifetime in the range of milliseconds, even in organic solvents, which implies a large TTA probability.[31] Third, its electronic structure prevents the generation of high-energy triplets upon TTA, thus maximizing the efficiency of the annihilation step.[15,16,19]

As introduced above, phosphorescent metalated porphyrins are used for TTA sensitization.[32] Thanks to the central heavy-metal ion, they show fast intersystem crossing. Therefore, after photo-excitation singlet states relax quickly into triplets, from which the energy is transferred to the optically dark triplets of the emitters. The absorption spectrum of metalloporphyrins is usually composed of two main peaks, the so-called *B*- (high energy) and *Q*- (low energy) bands,[33] separated by a transparency window of up to 200 nm wide, that can easily match the upconverted emission. Of course, only the *Q*-band is exploited in sTTA-UC, while the *B*-band sets the maximum UC gain achievable in the photon energy shift before having the re-absorption of the converted emission. This outline of sTTA-UC chromophore properties provides the guidelines for preparing an ideal broadband upconverting multisensitizer system. The *Q*-bands of different light-harvesters must be shifted progressively to broaden the overall absorption band. The corresponding phosphorescence peak should not move significantly in order to maintain the resonance with emitter triplets. In addition, the high energy *B*-bands should be unchanged to maintain a transparency window large enough to avoid the re-absorption.

Unfortunately, the synthesis of this set of porphyrins is not an easy task. The Goutermann model states that the porphyrinic peculiar electronic structure is determined by the properties of the two top-filled and two lowest empty π orbitals of the aromatic ring, whose combination results in the generation of the well-known absorption band profile.[32] Intensity changes and energy shifts of the absorption derive from changes in the conjugation length or the delocalized charge density on the ring. Accordingly, the electronic spectra depend on the peripheral substituent groups and axial ligands, the type of central metal ion, the fusion of aromatic molecules and the extent and deformation of the ring itself.[25,33,34] The most efficient strategy to red-shift the porphyrin absorption is to condense the phenyl groups on the central ring pyrroles, as demonstrated by the work of Yakutkin.[33] However, the standard symmetric condensation of four benzenes induces a large red-shift of all electronic energies, thus moving both *Q* and *B* absorption bands.[36] We have overcome this problem by synthesizing a series of asymmetric naphthobenzoporphyrins. In that case, the perturbation of the central ring is limited, allowing a continuous changing of the absorption peaks position. Most importantly, the asymmetric condensation plays an important role in determining the symmetry of the Goutermann orbitals. As suggested by Kobayashi and Konami calculations and demonstrated by Svagan et al., this strategy allows tuning the *Q*-band position while keeping the *B*-band almost unchanged.[30,35]

Figure 2 depicts the molecular structure and absorption spectra of the complete set of synthesized light-harvesters (see Experimental Section and Supporting Information). It includes a Pt(II)-*meso*-tetra(4-fluorophenyl)tetrabenzoporphyrin (PtTPTBPF) and three derivatives (Pt1N, Pt2N, Pt3N) obtained by progressive condensation of naphthalene on the macrocycle in order to continuously shift the absorption towards low energies. All these dyes show the typical absorption spectrum of the porphyrins (Figure 2b–d), with two well-separated absorption

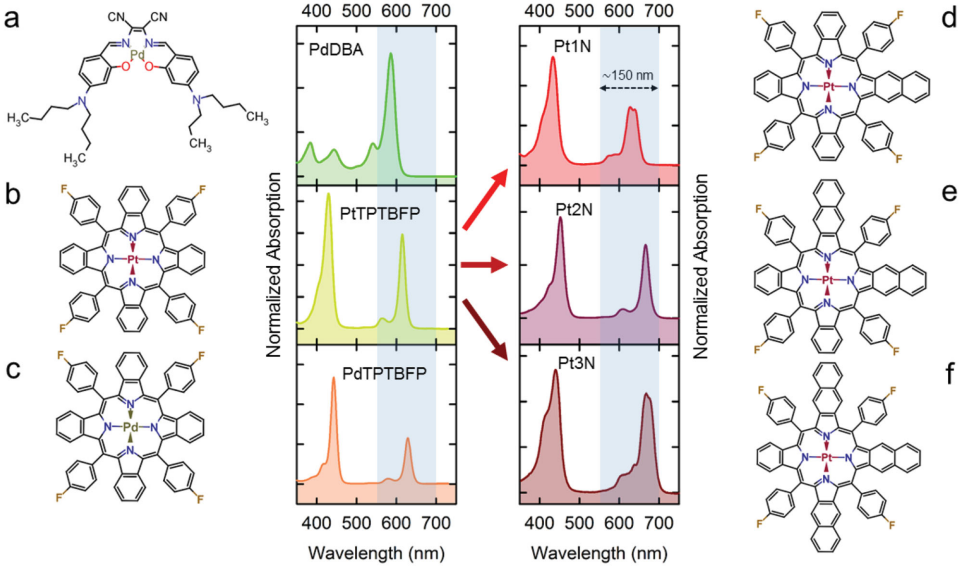

Figure 2. Molecular structures of the sensitizers used in the broadband-absorption sTTA-UC system. All the dyes are phosphorescent in the NIR, with emission wavelengths between 770 and 870 nm. The blue stripe shows the spectral range spanned by their long-wavelength absorption peaks. By several sensitizers we can broaden the overall absorption band of the system up to 150 nm.

maxima in the blue (the *B*-band) and in the red (the *Q*-band).[25,32] However, while the *B*-band is nearly fixed around 440 nm, the *Q*-band peak moves from 630 (PtTPTBPF) to 670 nm (Pt3N). In order to complete the spanned absorption range, the set of sensitizers has been integrated with two additional dyes: the Pd(II)-*meso*-tetra(4-fluorophenyl)tetrabenzoporphyrin (Figure 2c), where the *Q* band is bathochromically shifted in comparison to Pt(II) analogues because of the different effects of the central ion, and a donor–acceptor Schiff base (palladium(II) 2,3-bis[(4-dibutylamino-2-hydroxybenzylidene)-amino]but-2-enedinitrile, PdDBA). The latter also allows harvesting of the light at wavelengths shorter than 600 nm (Figure 2a) thanks to a complex absorption structure with a well-defined maximum at 585 nm and only few very weak absorption peaks in the UV–blue region. It should be noted that the transparency window of all the sensitizers matches the photoluminescence spectrum of perylene (see Figure 1b).[36]

The effective ability of the prepared sensitizers to excite the perylene triplet state has been studied in tetrahydrofuran (THF) solution by continuous wave and time-resolved photoluminescence measurements (see Experimental Section). In particular, we monitored the sensitizer photoluminescence spectra and yields, the intersystem crossing efficiency ϕ_{ISC} and, after addition of the emitter at suitable concentrations, the energy transfer yield ϕ_{ET} (see Table T1, Supporting Information). We found that all sensitizers have a ϕ_{ISC} close to one and show phosphorescence in the near-infrared, with emissions peaking between 770 and 870 nm, i.e., resonant with the perylene triplet at ≈800 nm.[31,37] However, the observed ϕ_{ET} is not the same for all light harvesters. When levels are perfectly resonant, the occurrence of an unavoidable back-ET from emitters to sensitizers can only partially be controlled by changing the relative dye concentration. This effect is even more evident when the sensitizer triplet state lies slightly below the triplet state of the emitter.[38,39] Therefore, the ideal condition for maximizing ϕ_{ET} is when the sensitizer triplet level is slightly above that of the emitter. Ttime-resolved phosphorescence measurements of the six sensitizers, discussed in detail in Figure S4 of the Supporting Information, shows the occurrence of all the behavior described above. With a perylene concentration as large as 10^{-3} M, we obtained an ET efficiency of larger than 95% for PdDBA, PtTPTBPF, and PdTPTBPF. In the case of Pt1N, ϕ_{ET} is still as large as 55%, whereas for the remaining dyes it settled at around 20–30%. By considering the spectral coverage of each compound, and in order to avoid that the system becomes unnecessarily complex, we restricted our investigations in the following experiments to mixtures of PtTPTBPF (8.6×10^{-5} M), PdDBA (7.9×10^{-5} M), Pt1N (8.5×10^{-5} M) and perylene (10^{-3} M), which offers a good ϕ_{ET} and ϕ_{ISC}, as well as a broad and uniform absorption across the entire range from 550 to 650 nm. In the next section, the sTTA-UC performances of this multisensitizer system are discussed in detail.

3. Efficiency of Broadband sTTA-UC

For application in real devices, instead of considering the classic QY_{UC}, it is more convenient to introduce an effective upconversion yield ϕ_{eff}, defined as the ratio between the number of converted photons and the number of incident ones. It can be written as a function of the excitation intensity I_{exc} and of the system harvesting efficiency ϕ_{harv},

$$\begin{aligned}\phi_{eff}(I_{exc},\phi_{harv}) &= QY_{UC}(I_{exc},\phi_{harv})\phi_{harv} \\ &= 0.5 f \phi_E \phi_{TTA}(I_{exc},\phi_{harv})\phi_{harv}\end{aligned} \quad (1)$$

where the factor 0.5 takes into account that two photons are required to produce one photon at higher energy. f is the statistical probability to obtain an excited singlet state upon annihilation of two triplets, which is a fixed parameter characteristic of the emitter, ϕ_E is the emitter fluorescence efficiency, and ϕ_{TTA} is the TTA yield.[39] As outlined in Equation (1), ϕ_{TTA} is a function of both I_{exc} and ϕ_{harv} because it results from the competition between the triplet spontaneous decay and decay due to reciprocal annihilation, which is in turn determined by the density of excited states. At the limit of high excitation intensity, i.e., when we can assume that all triplets decay by annihilation, ϕ_{TTA} becomes equal to one. Under this condition ϕ_{eff} is independent from I_{exc}, and is limited only by the light-harvesting capability of the system:

$$\begin{aligned}\lim_{I_{exc}\to\infty}\phi_{eff}(I_{exc},\phi_{harv}) &= 0.5 f \phi_E \phi_{harv} \\ &= 0.5 f \phi_E \underbrace{\bar{\alpha}\phi_{ISC}\phi_{ET}}_{\phi_{harv}}\end{aligned} \quad (2)$$

Here, $\bar{\alpha}$ is the fraction of incident photons absorbed by the sensitizer, i.e., the wavelength-integrated absorptance (see Supporting Information for details). As previously introduced, to quantify the irradiance at which the high excitation limit starts for sTTA-UC we must consider the excitation intensity threshold I_{th}, which is the power density at which ϕ_{TTA} is 0.5, which can be written as[24]

$$I_{th} = \frac{Z}{(\bar{\alpha}/d)\phi_{ISC}\phi_{ET}} \quad (3)$$

where d is the sample thickness, and Z is a parameter that is dependent on the emitter triplet decay and annihilation cross-sections as well as the diffusion constant of the energy/molecules in the system. Equations (2) and (3) indicate the main route to achieve large conversion efficiencies at low excitation power, as required for use in solar technology. If we consider sensitizers with $\phi_{ISC} = 1$, and once ϕ_{ET} has been maximized by a proper choice of the emitter concentration, further enhancements of ϕ_{eff} at low power can be obtained by incrementing $\bar{\alpha}$. However, it is worth pointing out that $\bar{\alpha}$ cannot be raised simply by increasing the sensitizer concentration (C_{sens}). Indeed, the molar absorption coefficient of common sensitizers is so large that for $C_{sens} > 10^{-4}$ M the incident light within their absorption band is completely harvested in an optical path of less than 0.1 cm.[25] Moreover, a high C_{sens} could lead to chromophore aggregation and enhance back-ET from the emitter to the sensitizer (see Figure S1, Supporting Information).[17] However, the simultaneous use of complementary sensitizers allows significant increases of $\bar{\alpha}$ by broadening the absorption band, without having issues that result from from a high C_{sens}. As a figure of merit of the multisensitizer's sTTA-UC effectiveness, we define the light-harvesting gain

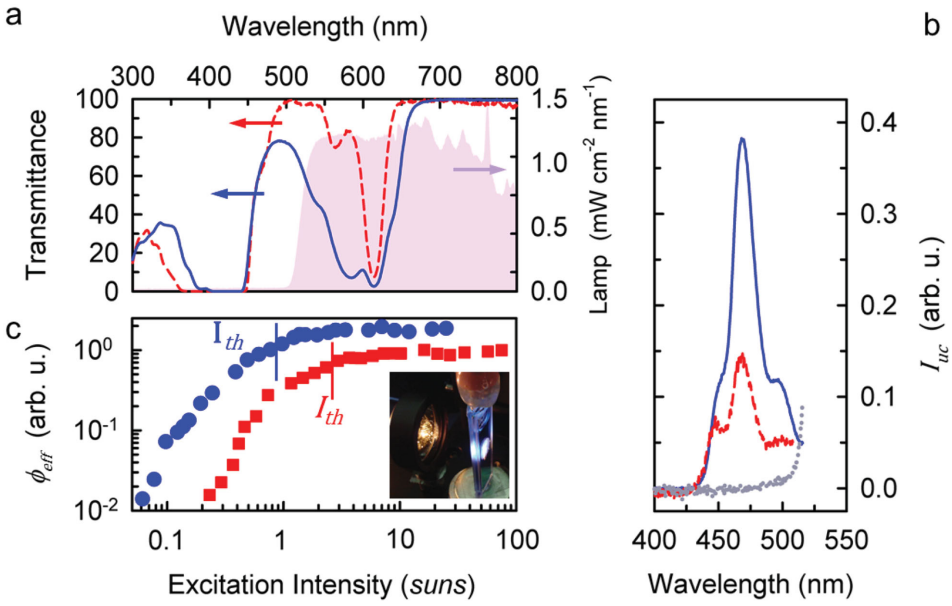

Figure 3. Optical properties of the described multisensitizer sTTA-UC. a) Transmittance profile of a single- (PtTPTBPF:perylene, red dashed line) and of a multi- (PtTPTBPF:PdDBA:Pt1N:perylene, blue solid line) sensitizers TTA-UC solution in THF (optical path = 0.1 cm). The shaded pink spectrum is the emission spectrum of the filtered xenon lamp, which was used as non-coherent source. b) Photoluminescence spectra of the single- (red dashed line) and multisensitizer (blue solid line) sTTA-UC systems at an excitation power density of 20 suns. Without the emitter, no upconverted light could be detected (dotted line). c) The relative conversion yield ϕ_{eff} measured as a function of the excitation intensity for the single- (squares) and multisensitizer (dots) upconverters. The data are normalized to the high excitation limit value of the single sensitizer solution. The inset is a picture of the sample under 10 suns of broadband excitation.

factor η as the ratio between the multisensitizer harvesting ability $\bar{\phi}_{harv}$ and the single sensitizer harvesting ability ϕ_{harv}. In the case of negligible overlap between sensitizer absorptions (see Supporting Information for details), the equation can be written as

$$\eta = \frac{\bar{\phi}_{harv}}{\phi_{harv}} = \frac{\sum_i \bar{\alpha}_i \phi_{ISC}^i \phi_{ET}^i}{\bar{\alpha}_i \phi_{ISC} \phi_{ET}} \quad (4)$$

where the sum index i runs over the full set of sensitizers. Equations (2)–(4) predict that ϕ_{eff} and I_{th} must be proportional and inversely proportional to η, respectively.

On this basis, we studied the multi-sensitizer system ϕ_{UC} as function of the excitation intensity I_{exc}. In particular, real-word operating conditions were reproduced by exciting the samples with a properly filtered xenon lamp to simulate the irradiance and emission profile of solar light after going through a SC device with an absorption edge at 540 nm.[7,40] **Figure 3** compares the excitation light spectrum with the transmittance of single/multisensitizers. Calculating the respective wavelength-integrated absorptance (Figure 3a), we obtain a light-harvesting gain of $\eta \approx 3$, which implies an expected enhancement (reduction) of ϕ_{eff} (I_{th}) of the same magnitude. Figure 3b shows the photoluminescence spectra of the sample excited at the high excitation limit (irradiance = 20 suns). Perylene luminescence is clearly observable, with its maximum at 470 nm. The converted light intensity I_{UC} of the multisensitizer system remarkably is ≈2.2 higher than that emitted by the single sensitizer, which does not deviate much from the value predicted by Equation (4), confirming the enhanced $\bar{\phi}_{harv}$ ability obtained by the co-presence of many absorbing species. The measurements of the I_{UC} dependency on the excitation irradiance are even more interesting (Figure 3c). The graph in Figure 3c shows the relative upconversion efficiency ϕ_{eff} for both samples on a log–log scale. For both samples, ϕ_{eff} follows linearly the excitation intensity at low powers, and then saturates becoming independent of the excitation above the respective power thresholds.[24] In the case of the single sensitizer solution, the slope change occurs at $I_{th} = 2.1 \times 10^{17}$ ph cm^{-2} s^{-1}, while for the multisensitizer solution we measure a three-fold reduction of the threshold, $I_{th} = 6.5 \times 10^{16}$. By considering the solar power distribution under AM 1.5 global conditions, the I_{th} value measured for the multisensitizer system corresponds to a sub-solar irradiance (0.9 suns). This is the lowest value observed for a fully organic sTTA-UC system, definitively demonstrating the suitability of this photon managing process for SC technologies.

It is interesting to note that, while the observed decrease of I_{th} exactly matches the value predicted by the theory, the experimental increase of ϕ_{eff} is smaller than the expected increase. In Equations (2) and (3), the only parameter affecting ϕ_{eff}, and not I_{th}, is the emitter quantum yield, thus suggesting a reduction of the fluorescence/light-collection efficiency of perylene in the multicomponent system despite that the same emitter concentration was used in both cases. Indeed, in the high excitation regime we measured a conversion yield of $QY_{UC} = 21\%$ for the multisensitizer system instead of the 33% reported for the model single-sensitizer solution (see Supporting Information, Figure S6).[19] This is due to a partial overlap between the low-energy tail of the multisensitizer *B*-bands and the upconverted perylene photoluminescence, which induces both self-absorption and resonant back ET from the emitters to the sensitizers. By

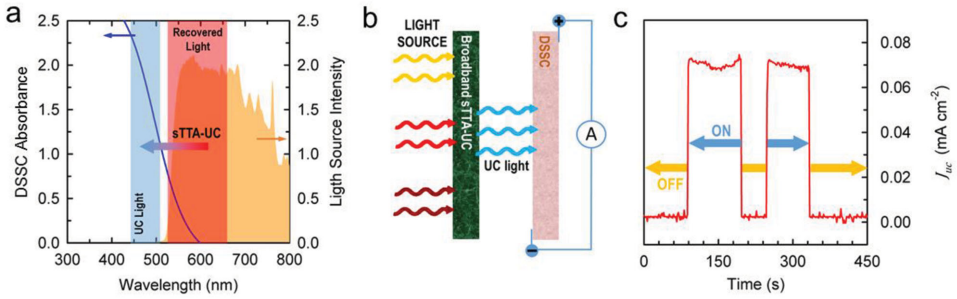

Figure 4. Test of the broadband sTTA-UC coupled to a research-grade DSSC. a) Absorbance of the DSSC cell (solid line) and emission spectrum of the filtered white lamp employed as light source. Colored stripes outline the working range of the tested broadband sTTA-UC. The red line shows the spectral range of the recovered sub-bandgap photons, while the blue line shows the upconverted emission range matching the DSSC absorption. b) Sketch of the experimental setup. c) Photocurrent generated in DSSC devices with (*ON* state) and without (*OFF* state) the upconverter.

comparing the shapes of the UC spectra reported in Figure 3b, it is evident that the low energy tail of the multisensitizer system is strongly reduced in respect with that of the single sensitizer one. The missing emission, due to self-absorption of the UC photoluminescence, corresponds to about one third of the observed yield reduction while the remaining fraction of the yield loss must be ascribed to an emitter-to-sensitizer Förster back ET.

Finally, it is important to note that, due to the reduction of I_{th} at 0.9 suns and broadband absorption, the 21% of maximum sTTA-UC quantum efficiency corresponds to a QY_{UC} at one sun as large as 10% (Figure S6 of the Supporting Information), which is a value about three times higher than that of the standard bi-component system (Figure 3c).

4. Application of Broadband sTTA-UC to a DSSC Cell

In order to demonstrate that sTTA-UC is able to produce light suitable for a SC, we coupled the system described in the previous session to a research-grade DSSC (**Figure 4**). Figure 4a shows the absorption spectrum of the employed cell, which begins to be transparent at wavelengths longer than about 550 nm (blue solid line). Therefore, the use of a Xe lamp filtered at 540 nm as excitation source (orange shaded spectrum) ensures that only the upconverted photons can be exploited in the current generation. By using the experimental set-up sketched in Figure 4b, we measured the current produced in the cell under a bias voltage of 0.8 V with (*On* state in Figure 4c) and without (*Off* state in Figure 4c) the broadband upconverter. The data reported in Figure 4c confirm that the DSSC does not work without the converter, but it supplies a short-circuit current density J_{uc} = 65 μA cm^{-2} at an irradiance of 7 suns when the sub-bandgap photons are upconverted into blue ones. When our DSSC was illuminated with unfiltered white light, it produces a current density of J_0 = 5.74 mA cm^{-2} (see Supporting Information, Figure S7); the gain $\xi = (J_{uc} + J_0)/J_0$ in the photocurrent generation corresponds to more than 1%, matching the performance of similar systems obtained at much higher irradiances.[12,22,41] Under 1 sun excitation, the photocurrent by UC drops to ≈30 μA cm^{-2}. As expected, the gain achievable by TTA-UC is lower, but still a measurable value. It is worth pointing out that ξ could be significantly enhanced by optimizing the optical coupling between the solar cells and the upconverting layer, which in our case was very poor, i.e., by using efficient solid-state TTA-UC materials mechanically coupled to the cell.

5. Conclusions

In conclusion, we have demonstrated how to obtain efficient, broadband sTTA-UC at sub-solar irradiance by enhancing the system's light-harvesting ability by using an ad-hoc synthesized family of sensitizers with complementary absorption properties. The simultaneous use of many harvesters allowed a significant extension of the system's spectral absorption coverage. Using our new approach the system absorptance has effectively been boosted achieving two important advantages. First, the number of solar-spectrum photons that are upconverted is doubled. Second, the irradiance required to obtain the maximum sTTA-UC yield is lowered by a factor of three. This way, we eliminated one of the main intrinsic limitations of sTTA-UC systems in which the use of classical sensitizers with narrow absorption bands implies the need for super-solar irradiance. The obtained photon upconversion yield of 10% under AM 1.5 broadband conditions strengthens the position of the sTTA-UC as the most promising photon managing strategy for application in solar-based devices.

6. Experimental Section

Sensitizer Synthesis: All light-harvesting chormophores (PdDBA[42]; PtTPTBPF and PdTPTBPF[43]; Pt1N, Pt2N, and Pt3N[44] were prepared according to previously published procedures.

Photoluminescence Studies—Optical Absorption: Absorption spectra of chromophore solutions in anhydrous tetrahydrofuran (THF, >99.9%, inhibitor free from Sigma-Aldrich) were recorded with a Cary Varian 50 spectrophotometer at normal incidence in a quartz cuvette with a thickness of 0.1 cm.

Photoluminescence Studies—Upconversion Continuous Wave and Time-resolved Photoluminescence: QY_{UC} was measured by comparison with a standard sTTA-UC system. Perylene (10^{-3} M) and palladium(II) *meso*-tetra(4-fluorophenyl)tetrabenzoporphyrin (10^{-5} M) were used as the emitter and sensitizer, respectively, in THF solution. This sTTA-UC system shifts photons from the red (≈632 nm) to the blue (≈475 nm) resulting

in an effective upconversion maximum QY_{UC} of ≈33%.[19] All solutions were prepared and sealed in a glove box under nitrogen atmosphere in order to prevent quenching of the involved triplet states by molecular oxygen. Photoluminescence spectra were recorded by a nitrogen-cooled CCD coupled with a Triax-190 spectrograph (Horiba Jobin-Yvon) with a spectral resolution of 0.5 nm. As excitation source a filtered high-pressure xenon lamp was used. The source irradiance was measured by a Thorlabs S302C thermal power sensor. To proof the energy transfer towards emitter molecules, the sensitizer's photoluminescence was studied by continuous wave and time-resolved techniques. As excitation source, we used a Roithner solid-state laser diode RLTMRL-635–100–5 at 1.95 eV (635 nm). For time-resolved studies, the source has been modulated by using a TTi TG550 wave function generator. The photoluminescence decay in time has been recorded in photon-counting mode using a Hamamatsu R943–02 photomultiplier connected to an Ortec 9353 multichannel scaler, with an overall time resolution of less than 3 ns.

DSSC Cell Preparation and Characterization—Dye Synthesis: The synthesis of the organic dye employed as light harvester for the model DSSC, namely the (*E*)-2-cyano-3-(5-(4-(diphenylamino)phenyl)thiophen-2-yl)acrylic acid (TTCA), was carried out as described in the literature, i.e., by palladium-catalyzed Suzuki coupling or direct arylation of the suitable and commercially available reagents (see Supporting Information for details).[45] All reactions were performed using standard glass vessels under an inert nitrogen atmosphere. All solvents were purchased from Sigma Aldrich and, unless otherwise specified, they have been used without further purification. ^{1}H NMR spectra were recorded on a 400 MHz Avance (Bruker) in CD_2Cl_2 as solvent, reference peak: δ(1H) = 5.30 ppm. DCI-MS analysis was carried out on a Finnigan Mat 95S magnetic mass spectrometer by loading a drop of sample solution in CH_2Cl_2 on the metal emitter placed on the top of a direct insertion probe.

DSSC Cell Preparation and Characterization—Device Fabrication: The fabrication of the devices was performed by conventional techniques.[46] TiO_2 electrodes were prepared by spreading (doctor blading) a colloidal TiO_2 paste (20 nm sized; ''Dyesol" DSL 18NR-T) onto a conducting glass slide (FTO, Hartford glass company, TEC 8, having a thickness of 2.3 mm and a sheet resistance in the range 6–9 Ω cm^{-2}) that had been cleaned with water and EtOH, treated with a plasma cleaner at 100 W for 10 min, dipped in a freshly prepared aqueous $TiCl_4$ solution (4.5×10^{-2} M), at 70 °C, for 30 min, and finally washed with ethanol. After drying at 125 °C for 15 min, a reflecting scattering layer containing >100 nm sized TiO_2 (Solaronix Ti-Nanoxide R/SP) was bladed over the first TiO_2 coat and sintered at 500 °C for 30 min. Then, the glass-coated TiO_2 was dipped again into a freshly prepared aqueous $TiCl_4$ solution (4.5×10^{-2} M), at 70 °C for 30 min, washed with ethanol, and heated once more at 500 °C for 15 min. At the end of these operations the final thickness of the TiO_2 electrode was in the range 8–12 μm, as determined by SEM analysis. After the second sintering, the FTO glass-coated TiO_2 was cooled at about 80 °C and immediately dipped into a dichloromethane solution (5×10^{-3} M) of the selected dye atroom temperature. for 24 h. The dyed titania-glasses were washed with EtOH and dried at room temperature under a N_2 flux. Finally, the excess of TiO_2 was removed with a sharp Teflon penknife and the exact active area of the dyed TiO_2 was calculated by means of microphotography. A 50 μm thick Surlyn spacer (TPS 065093–50 from Dyesol) was used to seal the photoanode and a platinized FTO counter electrode. Then the cell was filled up with the I^-/I_3^-electrolyte solution. Photocurrents were measured by a Keithley 2400 Picoammeter/Voltage Source.

sTTA-UC enhanced DSSC: The described DSSC cell was coupled to a broadband upconverting solution to demonstrate that the sTTA-UC produces photons that can enhance the PV performance. To this aim, a quartz cuvette of 0.1 cm thickness was filled with a THF solution (Sigma Aldrich, anhydrous, ≥99.9%, inhibitor-free) with PtTPTBPF (8.6×10^{-5} M), PdDBA (7.9×10^{-5} M), Pt1N (8.5×10^{-5} M) and perylene (10^{-3} M). The cuvette was placed in close contact with the front side of the DSSC by using a Cargille refractive index matching liquid to remove the air/quartz interface and improve the optical coupling between the upconverter and the cell. As excitation source, we used a high pressure xenon lamp filtered with a 540 nm long-pass colored filter. This way, the only photons that can be exploited by the DSSC to generate photocurrent are the blue ones produced by the sTTA-UC.

Supporting Information

Supporting Information is available from the Wiley Online Library or from the author.

Acknowledgements

This work was supported by funding from Eni Corporate – S.p.A, Divisione Energie Rinnovabili, Istituto Donegani (Novara). A.M. acknowledges support from Edison S.p.A. and Centro Volta for the Somaini Scholarship.
Note: Equation 2 and affiliations were corrected on September 16, 2015.

Received: June 19, 2015
Revised: July 17, 2015
Published online: August 25, 2015

[1] D. M. Chapin, C. S. Fuller, G. L. Pearson, *J. Appl. Phys.* **1954**, *25*, 676.
[2] M. A. Green, *Third Generation Photovoltaics: Advanced Solar Energy Conversion*, Springer, Berlin, Germany **2006**.
[3] D. Ginley, M. A. Green, R. Collins, *MRS Bull.* **2008**, *33*, 355.
[4] G. F. Nemet, *Energy Policy* **2006**, *34*, 3218.
[5] B. Kippelen, J.-L. Bredas, *Energy Environ. Sci.* **2009**, *2*, 251.
[6] V. Jankus, E. W. Snedden, D. W. Bright, V. L. Whittle, J. A. G. Williams, A. Monkman, *Adv. Funct. Mater.* **2013**, *23*, 384.
[7] A. Kudo, Y. Miseki, *Chem. Soc. Rev.* **2009**, *38*, 253.
[8] a) F. Meinardi, A. Colombo, K. A. Velizhanin, R. Simonutti, M. Lorenzon, L. Beverina, R. Viswanatha, V. I. Klimov, S. Brovelli, *Nat. Photonics* **2014**, *8*, 392; b) D. N. Congreve, J. Lee, N. J. Thompson, E. Hontz, S. R. Yost, P. D. Reusswig, M. E. Bahlke, S. Reineke, T. Van Voorhis, M. A. Baldo, *Science* **2013**, *340*, 334.
[9] a) T. Trupke, M. A. Green, P. Würfel, *J. Appl. Phys.* **2002**, *92*, 4117; b) J. de Wild, A. Meijerink, J. K. Rath, W. G. J. H. M. van Sark, R. E. I. Schropp, *Energy Environ. Sci.* **2011**, *4*, 4835; c) X. Huang, S. Han, W. Huang, X. Liu, *Chem. Soc. Rev.* **2013**, *42*, 173; d) S. Ji, J. Ge, D. Escudero, Z. Wang, J. Zhao, D. Jacquemin, *J. Org. Chem.* **2015**, *80*, 5958; e) C. Zhang, J. Zhao, X. Cui, X. Wu, *J. Org. Chem.* **2015**, *80*, 5674.
[10] T. Trupke, A. Shalav, B. S. Richards, P. Wurfel, M. A. Green, *Sol. Energy Mater. Sol. Cells* **2006**, *90*, 3327.
[11] a) J. de Wild, J. K. Rath, A. Meijerink, W. G. J. H. M. van Sark, R. E. I. Schropp, *Sol. Energy Mater. Sol. Cells* **2010**, *94*, 2395; b) G.-B. Shan, G. P. Demopoulos, *Adv. Mater.* **2010**, *22*, 4373.
[12] W. Zou, C. Visser, J. A. Maduro, M. S. Pshenichnikov, J. C. Hummelen, *Nat. Photon.* **2012**, *6*, 560.
[13] a) R. R. Islangulov, F. N. Castellano, *Angew. Chem. Int. Ed.* **2006**, *45*, 5957; b) S. Baluschev, T. Miteva, V. Yakutkin, G. Nelles, A. Yasuda, G. Wegner, *Phys. Rev.Lett.* **2006**, 97; c) T. F. Schulze, T. W. Schmidt, *Energy Environ. Sci.* **2015**, *8*, 103.
[14] T. W. Schmidt, F. N. Castellano, *J. Phys. Chem. Lett.* **2014**, *5*, 4062.
[15] Y. Y. Cheng, B. Fuckel, T. Khoury, R. Clady, M. J. Y. Tayebjee, N. J. Ekins-Daukes, M. J. Crossley, T. W. Schmidt, *J. Phys. Chem. Lett.* **2010**, *1*, 1795.
[16] Y. Y. Cheng, T. Khoury, R. Clady, M. J. Y. Tayebjee, N. J. Ekins-Daukes, M. J. Crossley, T. W. Schmidt, *Phys. Chem. Chem. Phys.* **2010**, *12*, 66.
[17] A. Monguzzi, R. Tubino, S. Hoseinkhani, M. Campione, F. Meinardi, *Phys. Chem. Chem. Phys.* **2012**, *14*, 4322.
[18] a) P. Duan, N. Yanai, N. Kimizuka, *Chem. Commun.* **2014**, *50*, 13111; b) Y. C. Simon, C. Weder, *J. Mater. Chem.* **2012**, *22*, 20817.

[19] S. Hoseinkhani, R. Tubino, F. Meinardi, A. Monguzzi, *Phys. Chem. Chem. Phys.* **2015**, *17*, 4020.
[20] P. Duan, N. Yanai, N. Kimizuka, *J. Am. Chem. Soc.* **2013**, *135*, 19056.
[21] P. Duan, N. Yanai, H. Nagatomi, N. Kimizuka, *J. Am. Chem. Soc.* **2015**, *137*, 1887.
[22] Y. Y. Cheng, B. Fuckel, R. W. MacQueen, T. Khoury, R. G. C. R. Clady, T. F. Schulze, N. J. Ekins-Daukes, M. J. Crossley, B. Stannowski, K. Lips, T. W. Schmidt, *Energy Environ. Sci.* **2012**, *5*, 6953.
[23] a) T. F. Schulze, J. Czolk, Y.-Y. Cheng, B. Fückel, R. W. MacQueen, T. Khoury, M. J. Crossley, B. Stannowski, K. Lips, U. Lemmer, A. Colsmann, T. W. Schmidt, *J. Phys. Chem. C* **2012**, *116*, 22794; b) A. Nattestad, Y. Y. Cheng, R. W. MacQueen, T. F. Schulze, F. W. Thompson, A. J. Mozer, B. Fückel, T. Khoury, M. J. Crossley, K. Lips, G. G. Wallace, T. W. Schmidt, *J. Phys. Chem. Lett.* **2013**, *4*, 2073; c) A. Monguzzi, F. Bianchi, A. Bianchi, M. Mauri, R. Simonutti, R. Ruffo, R. Tubino, F. Meinardi, *Adv. Energy Mater.* **2013**, *3*, 680; d) R. S. Khnayzer, J. Blumhoff, J. A. Harrington, A. Haefele, F. Deng, F. N. Castellano, *Chem. Commun.* **2012**, *48*, 209.
[24] A. Monguzzi, J. Mezyk, F. Scotognella, R. Tubino, F. Meinardi, *Phys. Rev. B* **2008**, *78*, 195112.
[25] D. Papkovsky, T. O'Riordan, *J. Fluoresc.* **2005**, *15*, 569.
[26] W. Shao, G. Chen, T. Y. Ohulchanskyy, A. Kuzmin, J. Damasco, H. Qiu, C. Yang, H. Ågren, P. N. Prasad, *Adv. Optical Mater.* **2015**, *3*, 575.
[27] D. M. Wu, A. García-Etxarri, A. Salleo, J. A. Dionne, *J. Phys. Chem. Lett.* **2014**, *5*, 4020.
[28] A. Monguzzi, D. Braga, M. Gandini, V. C. Holmberg, D. K. Kim, A. Sahu, D. J. Norris, F. Meinardi, *Nano Lett.* **2014**, *14*, 6644.
[29] S. Baluschev, V. Yakutkin, G. Wegner, T. Miteva, G. Nelles, A. Yasuda, S. Chernov, S. Aleshchenkov, A. Cheprakov, *Appl. Phys. Lett.* **2007**, *90*, 181103.
[30] A. J. Svagan, D. Busko, Y. Avlasevich, G. Glasser, S. Baluschev, K. Landfester, *ACS Nano* **2014**, *8*, 8198.
[31] M. Montalti, S. L. Murov, *Handbook of Photochemistry*, CRC/Taylor & Francis, Boca Raton, FL, USA **2006**.
[32] M. Gouterman, *J. Mol. Spectr.* **1961**, *6*, 138.
[33] V. Yakutkin, S. Aleshchenkov, S. Chernov, T. Miteva, G. Nelles, A. Cheprakov, S. Baluschev, *Chem. Eur. J. A* **2008**, *14*, 9846.
[34] J. R. Sommer, A. H. Shelton, A. Parthasarathy, I. Ghiviriga, J. R. Reynolds, K. S. Schanze, *Chem. Mater.* **2011**, *23*, 5296.
[35] N. Kobayashi, H. Konami, *J. Porph. Phthal.* **2001**, *5*, 233.
[36] J.-H. Kim, F. Deng, F. N. Castellano, J.-H. Kim, *ACS Photonics* **2014**, *1*, 382.
[37] R. H. Clarke, R. M. Hochstrasser, *J. Mol. Spectr.* **1969**, *32*, 309.
[38] Y. Y. Cheng, B. Fuckel, T. Khoury, R. Clady, N. J. Ekins-Daukes, M. J. Crossley, T. W. Schmidt, *J. Phys. Chem. A* **2011**, *115*, 1047.
[39] R. P. Groff, R. E. Merrifield, P. Avakian, *Chem. Phys. Lett.* **1970**, *5*, 168.
[40] M. Grätzel, *Inorg. Chem.* **2005**, *44*, 6841.
[41] T. F. Schulze, Y. Y. Cheng, B. Fückel, R. W. MacQueen, A. Danos, N. J. L. K. Davis, M. J. Y. Tayebjee, T. Khoury, R. G. C. R. Clady, N. J. Ekins-Daukes, M. J. Crossley, B. Stannowski, K. Lips, T. W. Schmidt, *Aus. J. Chem.* **2012**, *65*, 480.
[42] S. M. Borisov, R. Saf, R. Fischer, I. Klimant, *Inorg. Chem.* **2013**, *52*, 1206.
[43] S. M. Borisov, G. Nuss, W. Haas, R. Saf, M. Schmuck, I. Klimant, *J. Photochem. Photobiol. A: Chem.* **2009**, *201*, 128.
[44] F. Niedermair, S. M. Borisov, G. Zenkl, O. T. Hofmann, H. Weber, R. Saf, I. Klimant, *Inorg. Chem.* **2010**, *49*, 9333.
[45] a) M. Velusamy, K. R. Justin Thomas, J. T. Lin, Y.-C. Hsu, K.-C. Ho, *Org. Lett.* **2005**, *7*, 1899; b) D. P. Hagberg, T. Marinado, K. M. Karlsson, K. Nonomura, P. Qin, G. Boschloo, T. Brinck, A. Hagfeldt, L. Sun, *J. Org. Chem.* **2007**, *72*, 9550; c) W.-H. Liu, I. C. Wu, C.-H. Lai, C.-H. Lai, P.-T. Chou, Y.-T. Li, C.-L. Chen, Y.-Y. Hsu, Y. Chi, *Chem. Commun.* **2008**, 5152; d) D. J. Schipper, K. Fagnou, *Chem. Mater.* **2011**, *23*, 1594; e) C. Lelii, M. G. Bawendi, P. Biagini, P.-Y. Chen, M. Crucianelli, J. M. D'Arcy, F. De Angelis, P. T. Hammond, R. Po, *J. Mater. Chem. A* **2014**, *2*, 18375.
[46] S. Ito, T. N. Murakami, P. Comte, P. Liska, C. Grätzel, M. K. Nazeeruddin, M. Grätzel, *Thin Solid Films* **2008**, *516*, 4613.